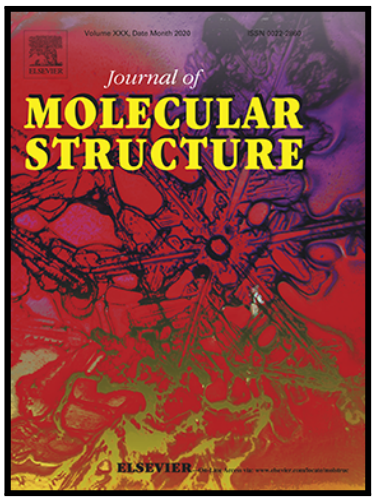

DNA Interaction Analysis with Automated Biosensor of Paraben Derivative s-Triazines

Elif Şenkuytu , Derya Davarcı , Zehra Ölçer ,
Gönül Yenilmez Çiftçi

PII: S0022-2860(20)31250-3
DOI: https://doi.org/10.1016/j.molstruc.2020.128925
Reference: MOLSTR 128925

To appear in: *Journal of Molecular Structure*

Received date: 29 March 2020
Revised date: 16 July 2020
Accepted date: 16 July 2020

Please cite this article as: Elif Şenkuytu , Derya Davarcı , Zehra Ölçer , Gönül Yenilmez Çiftçi , DNA Interaction Analysis with Automated Biosensor of Paraben Derivative s-Triazines, *Journal of Molecular Structure* (2020), doi: https://doi.org/10.1016/j.molstruc.2020.128925

Highlights

- **A series of paraben substituted s-triazine compounds were synthesized and characterized.**
- **DNA interaction studies of the compounds were performed with an automatic biosensor device.**
- **The benzyl paraben substituted s-triazine compound 5 was showed 61% and 75% activity reduction at concentrations 12.5 and 25 µM.**

DNA Interaction Analysis with Automated Biosensor of Paraben Derivative s-Triazines

Elif Şenkuytu[1,2], Derya Davarcı[2], Zehra Ölçer[2] and Gönül Yenilmez Çiftçi[2]*

[1]Department of Chemistry, Science of Faculty, Atatürk University, 25240, Erzurum, Turkey

[2]Department of Chemistry, Gebze Technical University, Gebze 41400, Kocaeli, Turkey

Corresponding author:

Dr. Elif Şenkuytu,

e-mail: elif.senkuytu@atauni.edu.tr ; Tel: +90 442 231 4441

ABSTRACT

Among all heterocyclic compounds, the triazine scaffold has an important place due to its wide range of biological activities. Triazine has been preferred by many researchers as the target structure for the design and development of new drugs, as it is found in many biologically active molecules with promising biological potential such as anti-inflammatory, anti-mycobacterial, anti-viral, anti-cancer properties. In this study, a series of paraben substituted s-triazine compounds **1**-**5** were synthesized and their structures were determined by ^{1}H and ^{13}C NMR spectroscopies as well as mass spectrometry. Also, structure of compound **5** was adjusted by X-ray crystallographic technique and crystallographic analysis revealed that **5** was crystallized in the trigonal space group *R*-3. According to X-ray analysis, compound 5 has very important intermolecular interaction such as nonclassical H-bond and pi-pi interaction. These interactions lead formation of supramolecular network. The thermal stabilities were investigated by thermogravimetric analysis. According to thermogravimetric analysis results, all of the synthesized compounds have high thermal stability. DNA interaction studies of the compounds **1-5** were performed with an automatic biosensor device that can measure the efficiency of DNA hybridization on the biochip surface. The biosensor results show that benzyl paraben substituted s-triazine compound **5**, the most reactive compound at low concentration, was showed 61% and 75% activity reduction at concentrations 12.5 and 25 µM.

Keywords: s-Triazine, Parabens, DNA Binding, Electrochemical Biosensor

Introduction

According to the World Health Organization (WHO), cancer disease, the second leading cause of death worldwide, is responsible for an estimated 9.6 million deaths in 2018. Globally, 1 out of 6 deaths (approximately 17% of all deaths) is due to cancer. Also, it is known that approximately 70% of cancer deaths occur in low- and middle income countries [1,2]. Parabens have been known for many years with their antimicrobial, antifungal properties and are widely used in the cosmetic and pharmaceutical industry [3,4]. Also, studies on the biological properties of parabens are frequently done [5,6]. In recent years, researchers have been great effort to identify molecules with anticancer properties from both natural and synthetic sources. Among the wide range of synthetic compounds known as potential anticancer drugs, molecules based on triazine scaffolds drew great attention [7,8].

One of the triazine isomers, s-triazine (1,3,5-triazine), is a symmetrical and six-membered nitrogen-containing heterocyclic compound. s-Triazine is a very useful scaffold for multifunctional molecular arrangements and a stepwise substitution reaction because it provides progressive substitution over three chlorine atoms [9-12]. s-Triazine has been used as starting compound for preparing of wide variety derivatives bearing the s-triazine moiety, due to the low-cost chemical, commercial availability, and easily substitution of the three chlorine atoms with many of nucleophiles under controlled temperature [13-18]. In addition, the chemical and physical properties of triazine derivatives can be modulated by the type, number and orientation of functional side groups [19-24] and substituted triazines are very stable, do not deteriorate under very aggressive chemical conditions. These fascinating compounds derived from triazine have been examined intensively and been the subject of many academic articles because of their widely applications in the pharmaceutical, cosmetic, textile, plastic industries. Triazine derivatives are used as pesticides, dyestuffs, optical

bleaches, explosives, and surface-active agents. Triazine derivatives have been studied especially in applications of medicinal chemistry [25-28]. The triazine scaffold provides the source for the design of biologically related molecules in many studies such as antileishmanial [29, 30], antimalarial [31], antimicrobial [32-34], antibacterial [35, 36], anticancer [37, 38] and antitumor [39, 40].

DNA (deoxyribonucleic acid) provides chemists a very powerful tool to monitoring a wide variety of diseases such as viral infections, infectious diseases. While molecules that damage DNA can cause cancer, their role as anti-cancer drugs is very important. Understanding of how molecules interact with DNA is important for the design of new drugs [41-43]. There are a lot of studies in literature have used biosensors for DNA interaction analysis and chemical toxicity tests [44, 45]. Electroanalytical techniques represent highly sensitive tools for determination of chemical carcinogen compounds or mutagens and their toxic effects on DNA [46, 47]. Although electroanalytical techniques have been proven to be a useful tool for genotoxicity tests, lack of automated and fast devices prevented its use as the routine toxicology analysis. Among the different detection methods, electrochemical DNA biosensors have been used effectively to study the interactions of DNA with various molecules [48, 49]. Moreover, due to the attractive advantages such as high sensitivity, low cost and minimum power requirements, electrochemical DNA biosensors are rapidly developing in clinical diagnosis and drug analysis areas. In this context, in the study, reactions of s-triazine with methyl-, ethyl-, propyl-, butyl- and benzyl-paraben were carried out in tetrahydrofuran, and fully paraben-substituted s-triazine compounds **1-5** were synthesized, respectively. The structures of s-triazine series compounds **1-5** were characterized by MALDI-TOF mass analysis, ^{1}H and ^{13}C NMR spectroscopies. Also, the solid-state structure and geometry of compound **5** was determined using single-crystal X-ray structural analysis. The thermal stability of compounds **1-5** were investigated by thermogravimetric analysis.

Biological activities and DNA interaction studies of the compounds **1-5** were also examined by automatic biosensor device.

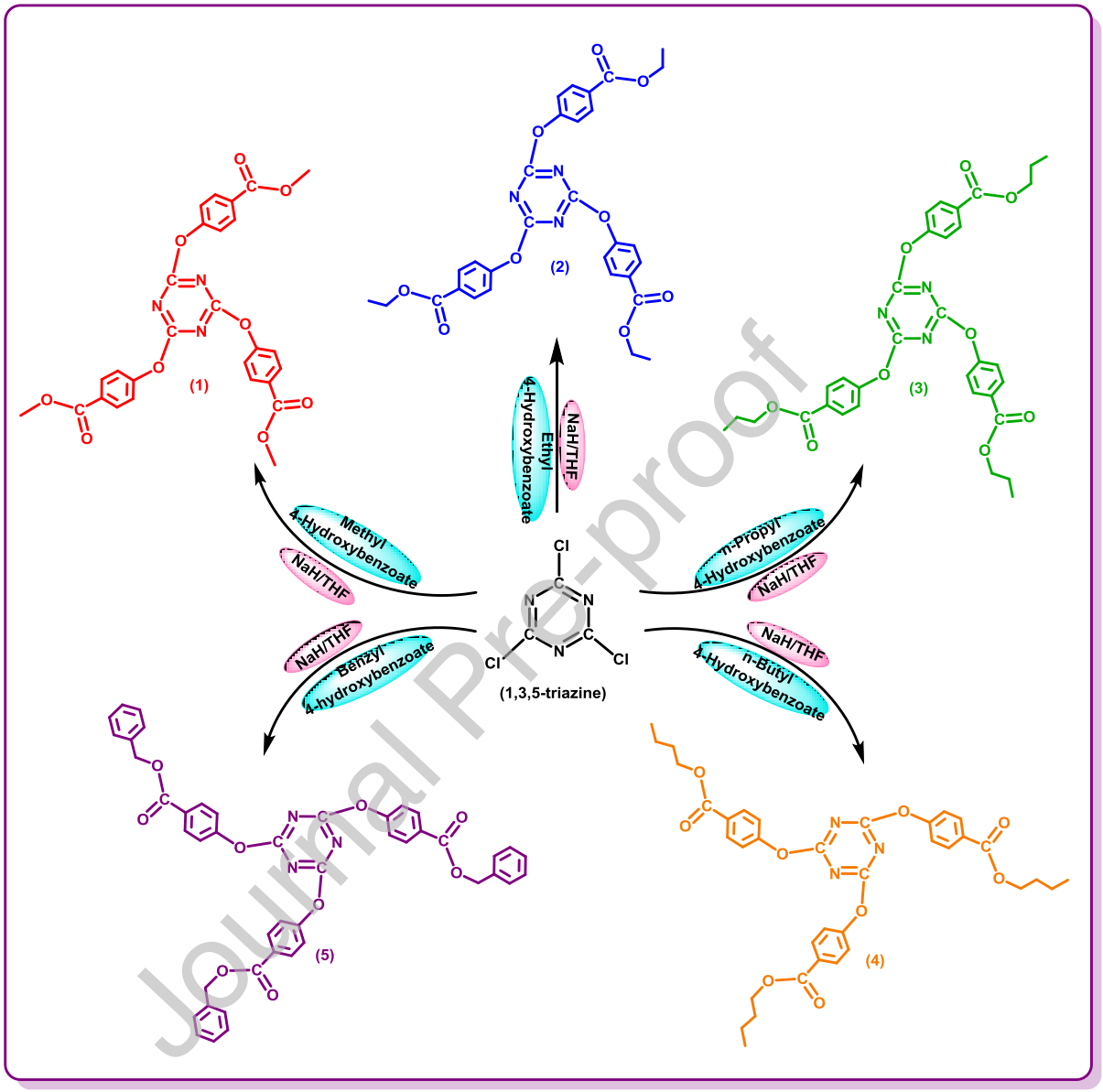

Scheme. Reactions of s-triazine with paraben derivatives

2. EXPERIMENTAL SECTION

2.1. General material and methods

1,3,5-s-triazine and paraben derivatives were obtained from Aldrich. Methyl 4-hydroxybenzoate (99.0%), ethyl 4-hydroxybenzoate (99.0%), n-propyl 4-hydroxybenzoate

(99.0%), n-butyl 4-hydroxybenzoate (99.0%) were obtained from Alfa Aesar and benzyl 4-hydroxybenzoate (99.0%) was obtained from Aldrich. Tetrahydrofuran (THF) (≥99.0%), dichloromethane (DCM) (≥99.0%), *n*-hexane (≥95.0%) were bought from Merck. THF was distilled over a sodium–potassium alloy under an atmosphere of dry argon. Silica gel 60 (230–400 mesh) for column chromatography was obtained from Merck. $CDCl_3$ for NMR spectroscopy was obtained from Goss Scientific. Positive ion and linear mode MALDI-MS of compounds were obtained in dihydroxybenzoic acid as MALDI matrix using nitrogen laser accumulating 50 laser shots using Bruker Microflex LT MALDI-TOF mass spectrometer. All reagents were purchased from Aldrich and used without further purification and all solvents were obtained from Merck. All reactions were monitored by thin layer chromatography using Merck TLC Silica gel 60 F_{254}. Silica gel 60 (particle size: 0.040-0.063 mm, 230-400 mesh ASTM) for column chromatography was obtained from Merck. All reactions were carried out under an argon atmosphere. ^{1}H and ^{13}C NMR spectra were recorded for all compounds in $CDCl_3$ solutions on a Varian INOVA 500 MHz spectrometer. Thermogravimetric analyses (TGA) were performed on a Mettler Toledo TGA/SDTA 851. Powder samples of the compounds were loaded into pans and heated at a ramp rate of 10 °C min^{-1} from room temperature to 700 °C under a N_2 atmosphere.

2.2. X-ray Crystallography

Suitable single crystals of compound **5** was carefully separated from other crystals in the crystallization vessel under a polarizing microscope and placed on a thin glass fiber using perfluoropolyether oil. The solid-state structures of the complexes were confirmed by X-ray crystallography. Data were obtained on a Bruker APEX II QUAZAR three-circle diffractometer using monochromatized Mo Kα X–radiation (λ = 0.71073 Å). Indexing was performed using APEX2 [50]. Data integration and reduction were carried out with SAINT [51]. Absorption correction was performed by multi-scan method implemented in SADABS

[52]. The structure was solved using SHELXT [53] and then refined by full-matrix least-squares refinements on F^2 using the SHELXL [54] in OLEX 2 program package [55]. All non-hydrogen atoms were refined anisotropically using all reflections with $I > 2\sigma(I)$. Aromatic and aliphatic C-bound H atoms were positioned geometrically and refined using a riding mode. Crystallographic data and refinement details of the data collection for **5** were given in Table S1. Crystal structure validations and geometrical calculations were performed using Platon software [56]. Mercury software [57] was used for visualization of the cif files. Additional crystallographic data with CCDC reference number (1964264 for **5)** has been deposited within the Cambridge Crystallographic Data Center *via* www.ccdc.cam.ac.uk/deposit.

2.3. Biochip, Biosensor device and DNA interaction tests

General information about biochip, biosensor device and DNA interaction tests were given in Supporting Information.

2.4. Synthesis

Synthesis methods of the compounds are very similar. Therefore, the details of the synthesis sections of the compounds were given in the supporting information.

Spectral data of compound 1: MS (MALDI-TOF) m/z (%): Calc. for ($C_{27}H_{21}N_3O_9$): 531.13; found 531.97 $[M]^+$ (Fig.S1). ^{1}H NMR, $CDCl_3$, 298 K: δ ppm, δ_H 7.86 (d, $^3J_{HH}$ = 8.75 Hz, 6H, Ha); 7.00 (d, $^3J_{HH}$ = 8.75 Hz, 6H, Hb); 3.93 (s, 9H, -OCH_3) (Fig.S2). ^{13}C NMR (126 MHz, $CDCl_3$, 293 K, δ ppm): 173.29(C_1), 166.02(C_6), 154.80(C_2), 131.27(C_4), 128.24(C_5), 121.38(C_3), 52.26(C_7) (Fig.S3).

Spectral data of compound 2: MS (MALDI-TOF) m/z (%): Calc. for ($C_{30}H_{27}N_3O_9$): 573.56; found 5734.46 $[M+H]^+$ (Fig.S4). ^{1}H NMR, $CDCl_3$, 298 K: δ_H ppm, 8.07 (d, $^3J_{HH}$ = 8.41 Hz,

6H, Ha); 7.21 (d, $^{3}J_{HH}$ = 8.41 Hz, 6H, Hb); 4.42-4.36 (m, 6H, -OCH_2); 1.43-1.38 (m, 9H, -CH_3) (Fig.S5). ^{13}C NMR (126 MHz, $CDCl_3$, 293 K, δ ppm): 173.09(C_1), 165.54(C_6), 154.72(C_2), 131.24(C_4), 128.59(C_5), 121.32(C_3), 61.15(C_7), 14.30(C_8) (Fig.S6).

Spectral data of compound 3: MS (MALDI-TOF) m/z (%): Calc. for ($C_{33}H_{33}N_3O_9$): 615.64; found 616.08 $[M+H]^+$ (Fig.S7). ^{1}H NMR, $CDCl_3$, 298 K: δ_H ppm, 8.08 (d, $^{3}J_{HH}$ = 8.53 Hz, 6H, Ha); 7.22 (d, $^{3}J_{HH}$ = 8.53 Hz, 6H, Hb); 4.41-4.27 (m, 6H, -OCH_2); 1.84-1.76 (m, 6H, -CH_2); 1.06-1.01 (m, 9H, -CH_3) (Fig.S8). ^{13}C NMR (126 MHz, $CDCl_3$, 293 K, δ ppm): 173.30(C_1), 165.60(C_6), 154.71(C_2), 131.25(C_4), 128.62(C_5), 121.33(C_3), 66.73(C_7), 22.09(C_8), 10.48(C_9) (Fig.S9).

Spectral data of compound 4: MS (MALDI-TOF) m/z (%): Calc. for ($C_{39}H_{39}N_3O_9$): 657.72; found 658.05 $[M+H]^+$ (Fig.S10). ^{1}H NMR, $CDCl_3$, 298 K: δ_H ppm, 8.07 (d, $^{3}J_{HH}$ = 8.67 Hz, 6H, Ha); 7.22 (d, $^{3}J_{HH}$ = 8.67 Hz, 6H, Hb); 4.36-4.31 (m, 6H, -OCH_2); 1.79-1.72 (m, 6H, -CH_2); 1.53-1.44 (m, 6H, -CH_2); 1.02-0.97 (m, 9H, -CH_3) (Fig.S11). ^{13}C NMR (126 MHz, $CDCl_3$, 293 K, δ ppm): 173.30(C_1), 165.59(C_6), 154.70(C_2), 131.26(C_4), 128.64(C_5), 121.33(C_3), 65.03(C_7), 30.74(C_8), 19.25(C_9), 13.74(C_{10}), (Fig.S12).

Spectral data of compound 5: MS (MALDI-TOF) m/z (%): Calc. for ($C_{45}H_{33}N_3O_9$): 759.77; found 759.06 $[M]^+$ (Fig.S13). ^{1}H NMR, $CDCl_3$, 298 K: δ_H ppm, 8.12 (d, $^{3}J_{HH}$ = 8.69 Hz, 6H, Ha); 8.75 (d, $^{3}J_{HH}$ = 6.70 Hz, 6H, -CH); 7.44-7.40 (m, 6H, -CH); 7.39-7.35 (m, 3H, -CH); 7.22 (d, $^{3}J_{HH}$ = 8.69 Hz, 6H, Hb); 5.37 (s, 6H, -OCH_2), (Fig.S14). ^{13}C NMR (126 MHz, $CDCl_3$, 293 K, δ ppm): 173.27(C_1), 165.34(C_6), 154.87(C_2), 135.85(C_8), 131.45(C_4), [128.62, 128.31, 128.25, 128.16 (C_5/C_9/ C_{10}/C_{11})], 121.42(C_3), 66.90(C_7) (Fig.S15).

3. RESULTS AND DISCUSSION

3.1. Synthesis and characterization of the compounds (1-5)

The synthesis of paraben-triazine compounds have been mentioned in a Patent [58]. The reported procedure uses toluene as the solvent and pyridine as the proton abstractor. To avoid the use of pyridine and also to replace high boiling toluene as solvent, we developed a new methodology for the synthesis of paraben substituted triazine compounds. In the current study, paraben substituted triazine compounds **1-5** were successfully synthesized and their synthesis strategies were summarized in Scheme. The potential biological properties of the parabens and paraben derivative compounds are known [59-62]. The triazine ring is very useful platform for preparing of new biological systems due to its ability to combining different functional groups. In these frameworks, reactions of 1,3,5-s-triazine with methyl-, ethyl-, propyl-, butyl- and benzyl paraben were then performed in the presence of sodium hydride and tetrahydrofuran to obtain full paraben substituted triazine compounds **1-5**. All the synthesized compounds were purified by column chromatography and each of the obtained compounds **1-5** was characterized by mass (MALDI-TOF), ^{1}H and ^{13}C NMR spectroscopies. The molecular structure of compound **5** was also determined by X-ray crystallography. The appropriate crystallographic data was reported in Table S1. The structure analysis data (mass, ^{1}H and ^{13}C NMR results) of the compounds are presented in the experimental section. Also, the spectral data of compounds **1-5** are given in the supporting file (Fig. S1-S31).

The ^{1}H NMR chemical shift-coupling constants of all protons and ^{13}C NMR chemical shifts of all carbons in the experimental part confirmed the structures of synthesized compounds **1-5**. In general, the aromatic and aliphatic protons for paraben-substituted triazines **1-5** were observed between 8.12-7.00 and 5.37-0.97 ppm, respectively. All integral values for compounds **1-5** confirmed the proposed structures. Also, while aromatic carbons of triazine compounds were observed between 173-121 ppm, aliphatic carbons were observed among 66-10 ppm in ^{13}C NMR spectra. The ^{1}H and ^{13}C NMR spectra of compound **4** was

depicted as an example in Fig 1a and 1b. While the -Ha and -Hb protons were observed as double peaks at 8.07 and 8.67 ppm, the -OCH_2 protons were seen as triple peaks at approximately 4.33 ppm. in addition, the -CH_2 and -CH_3 protons were observed as multiple peaks in the range of 1.79-1.44 ppm and as triple peaks at approximately 1.00 ppm, respectively (Fig. 2a).

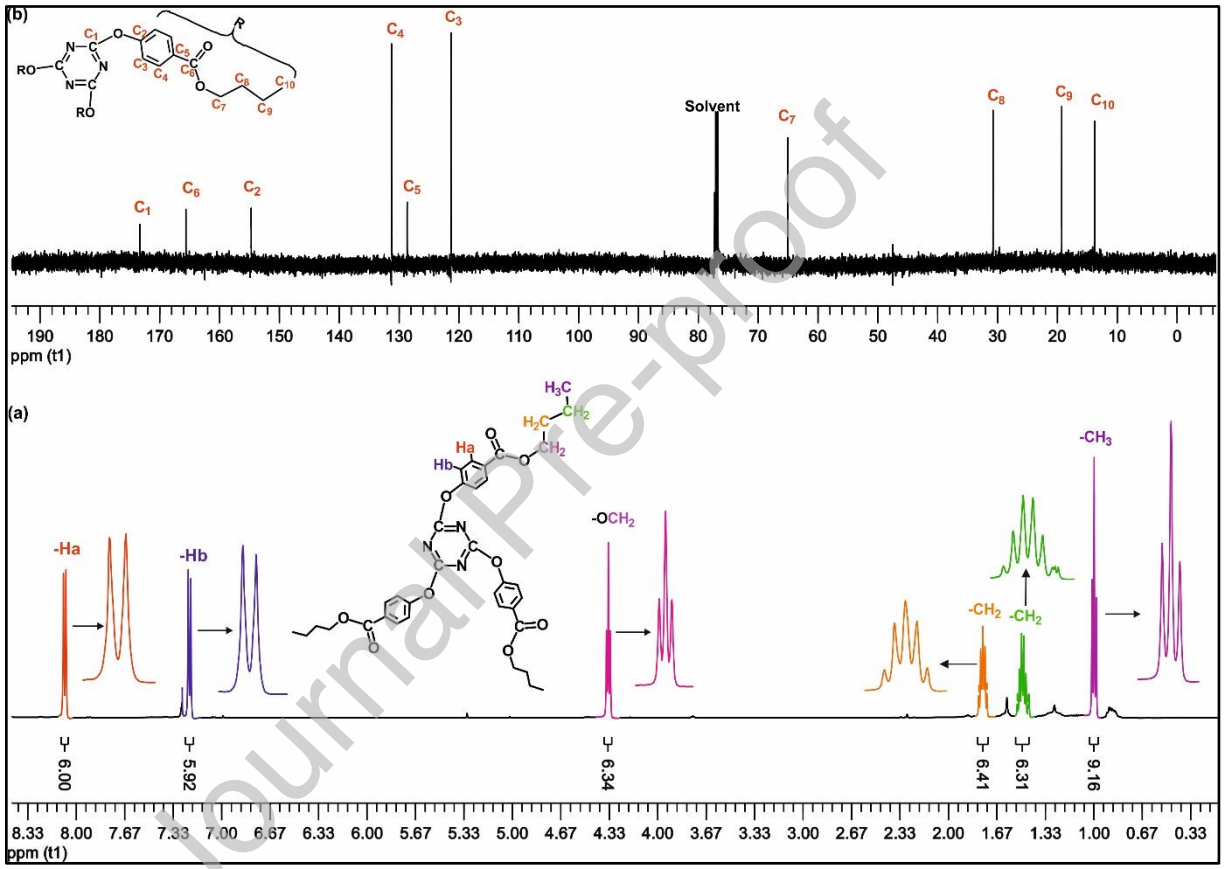

Figure 1. NMR spectra of the compound **4** in $CDCl_3$ solution (a) ^{1}H NMR spectrum and (b) ^{13}C NMR spectrum.

3.2. Thermal Stabilities of Compounds 1-5

All of the compounds were stable in air at room temperature. The thermal stability of the 1,3,5-s-triazine and paraben substituted triazine compounds (**1-5**) were investigated by determining the weight loss of a sample upon linearly increasing the temperature by conventional thermogravimetric analyses (TGA) at a heating rate of 10 °C/min up to 700 °C

under nitrogen flow. The thermal degradation curves of the compounds were given in Fig. 2. The weight loss of 99.5 % was observed at 154.6 °C for 1,3,5-s-triazine. Synthesized compounds **1- 5** have one-step thermal disruption curves. The compounds **1-5** were thermally stable at 370.9 °C, 401.6 °C, 394.2 °C, 381.5 °C, 414.5 °C and remained amounts of unspoiled were 22.1 %, 13.6 %, 7.7 %, 6.8 %, 17.6 %, respectively. The thermal stability of 1,3,5-s-triazine was lower than compounds **1**-**5**. According to thermogravimetric analyses, all of the synthesized compounds have high thermal stability and they are suitable for use in the construction of high temperature resistant organic materials.

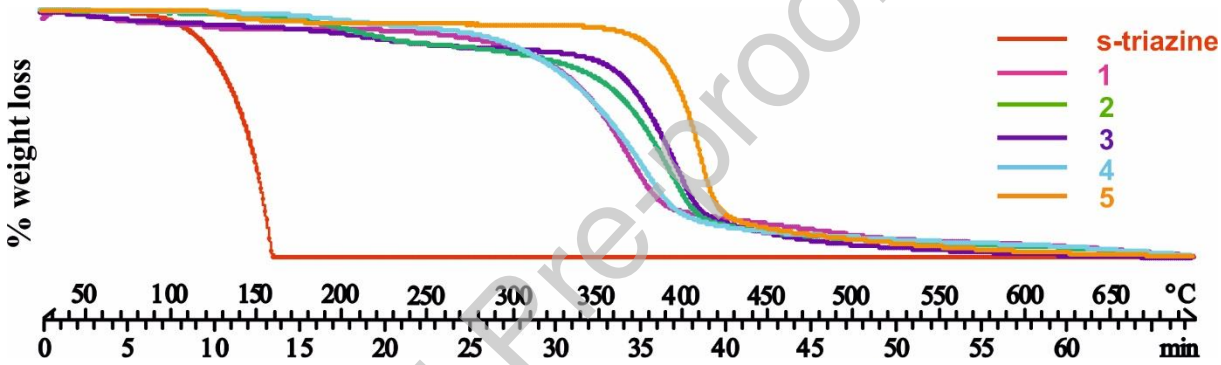

Figure 2. TGA curves of **1-5.**

3.3. Crystal Structure of Compound 5

The X-ray structure of compound **5** was consistent with those proposed on the basis of the NMR assignments. Crystallographic data, selected bond lengths and angles of compound **5** were summarized in Table S1-S3. Crystallographic analysis revealed that **5** was crystallized in the trigonal space group *R*-3. Compound **5** consist of a six-membered ring N_3C_3, which is fully substituted benzyl paraben on the C atoms (Fig. 3). As given in Table S2, the N1-C1^{i} and N1-C1 bond lengths are 1.333 (3) and 1.314 (3) Å; the N-C-N and C-N-C bond angles are 127.5 (2)°-112.5 (9)°, respectively. These values are typical for triazine derivatives [63-66]. Non-covalent interactions with H-bonds or aromatic clouds such as C-H···π, XH···π and π···π play an important role for formation of stable supramolecular network. It was seen that there

were some short interactions for compound **5** molecule and these values were given in Table S4a and 4b. As an example, 2D supramolecular structure like honeycomb (Fig. 4) formed through the *ab* plane via short interaction of C9-H9···π(Cg3) (Fig. 5). In addition, the strong aromatic interaction between the triazine rings along the *c* axis causes π···π stacking, which leads to formation of the 3D supramolecular network. The distance between the N_3C_3 rings (Cg1-Cg1) is 3.36 Å. (Fig 6).

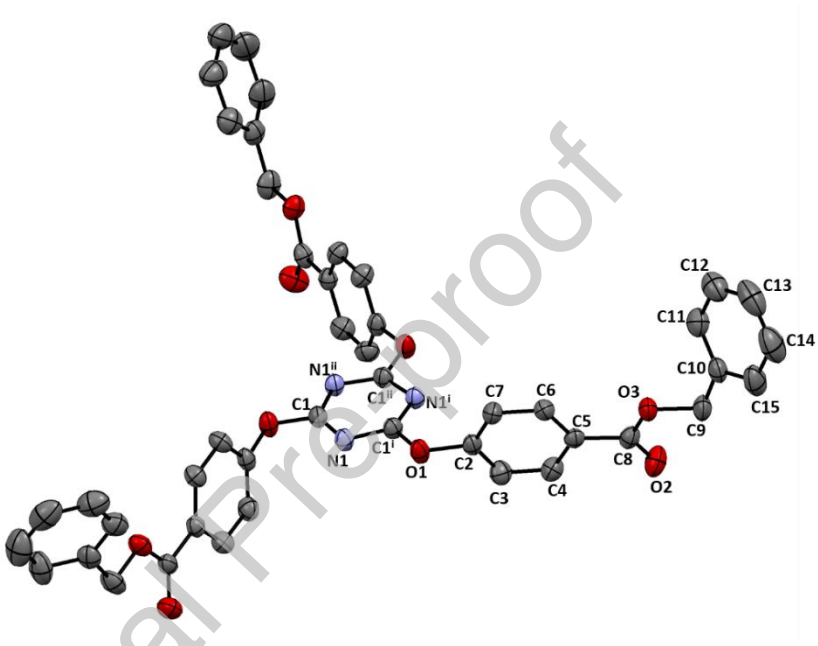

Figure 3. ORTEP drawing of compound **5** (30% probability level) The grey, blue and red coloured atoms represent C, N, O, respectively. All hydrogen atoms in **5** are omitted for clarity. (Symmetry codes: (i) −*x*+*y*+1, −*x*+1, *z*; (ii) −*y*+1, *x*−*y*, *z*.).

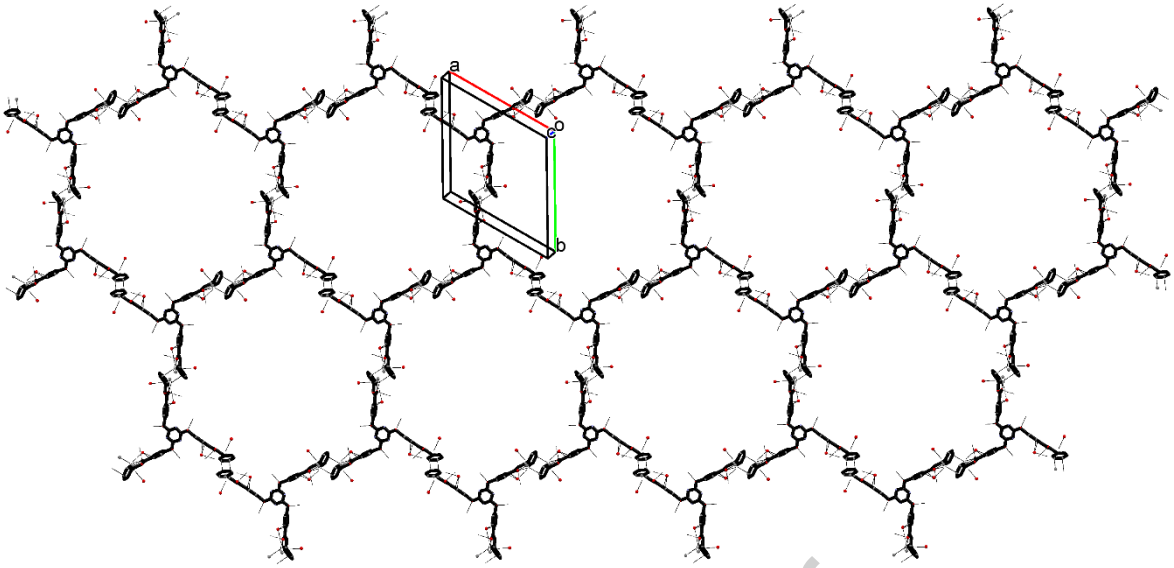

Figure 4. C9-H9A···Cg3 interaction caused like honeycomb 2D supramolecular network along the *ab* plane for compound **5**

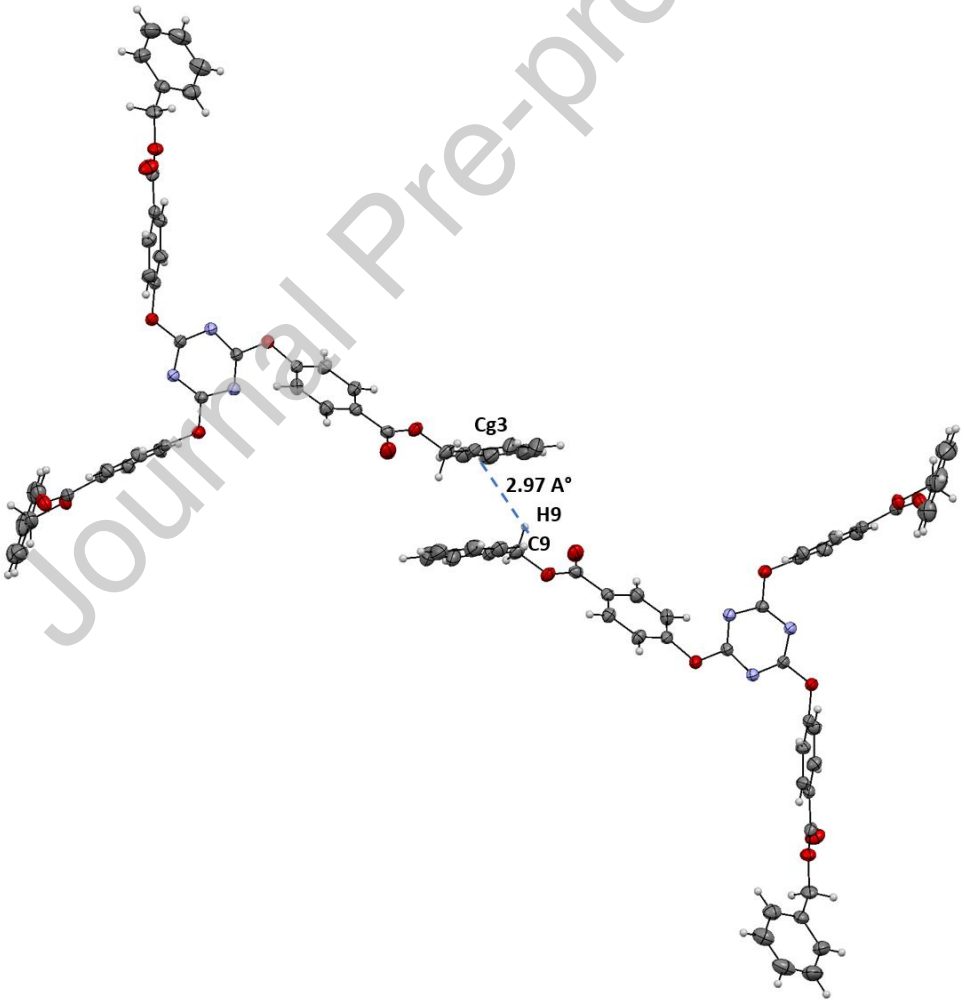

Figure 5. Perspective view of C9-H9···π (Cg3) intera2ction between compound **5** molecules

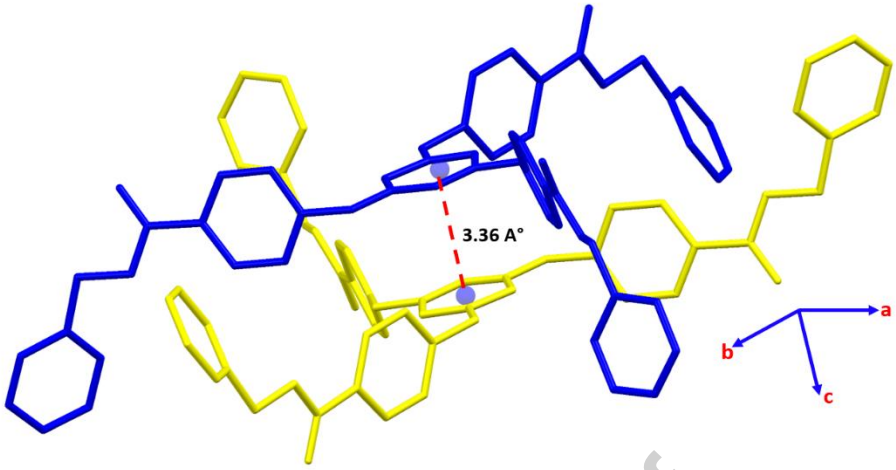

Figure 6. Perspective view of π···π stacking interaction (red dotted line) between N_3C_3 rings (Cg1 rings) along the *c* axix.

Puckering analysis is a measure of ring conformation. It is calculation of the mean plane and puckering parameters that afford a quantitative descriptor, the total puckering amplitude (Q) [67]. In compound **5**, N_3C_3 ring is almost planar (Fig. 7) and total puckering amplitudes for 6-membered-ring couldn't be analyzed (No C & P - Puckering Analysis since <Tau> = 0.1 < 5.0 Deg.) [68, 69]. Q_T values for N_3C_3 ring and deviations of nitrogen and carbon atoms from the ring plane are given in Table S3.

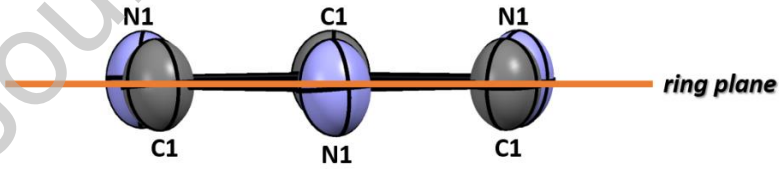

Figure 7. The conformation of N_3C_3 ring for compound **5**.

3.4. DNA Interaction Analysis with Automated Electrochemical Biosensor of the Compounds 1-5.

DNA interaction assays with paraben substituted *s*-triazine compounds **1-5** were carried out with MiSens® device, an automated electrochemical biosensor with sensitivity and fast response [70-72]. The interactions consist of several steps on microfluidic channel integrated

biochip during flow (Fig. S16). It was studied a successful alkanethiol coating on the biochip surface and the effect of the alkanethiol construction was measured using potassium ferrocyanide solution. In Fig. S17 showed that electrochemical reduction and oxidation area of ferrocyanide was larger on bare gold sensor chip than alkanethiol coated chip, and this evidenced the formation of self-assembled monolayer for the NeutrAvidin immobilization. For the investigation of synthesized compounds firstly, the biotinylated surface probe DNA was captured on Neutravidin immobilized biochip surface. Hybridized complementary target sequence and biotinylated detection probe DNA were incubated with varying concentrations (0-50 μM) of compounds and then this mixture was injected to the capture probe immobilized biochip surface in order to achieve the hybridization process of complementary surface probe (capture probe). In the next step, Neutravidin and HRP enzyme immobilized gold nanoparticles were injected to the biochip surface for binding via neutravidin and biotin interaction, and then an amperometric biosensor signal was measured during the substrate TMB injection (Fig. S18).

The individual reactive parabens (*methyl-, ethyl-, propyl-, butyl-, and benzyl-parabens*), 1,3,5-s-triazine and the paraben substituted *s*-triazine compounds **1–5** were tested by biosensor device and the hybridization activity results are shown Fig. 8 and Fig. S19 indicated by remaining from interaction and interacting DNA. While the individual parabens interact with DNA at a rate of 35-20%, it was observed that the substituted-s-triazine compounds **1-5** to which these parabens bind interact with DNA in approximately 70% at 50 μM concentration. Especially, when the hybridization activity of the synthesized products has been compared to parabens, they have shown the high activity reduction in low concentrations (12.5 and 25 μM) (Fig. 8 and Fig. S19). It was observed that among the synthesized compounds, benzyl-paraben substituted triazine (**5**) was the most reactive compound at low concentration. Compound **5** has shown 61% and 75% activity reduction in 12.5 and 25 μM

concentrations, respectively. At low concentration, 12.5 µM, compounds **2, 3,** and **4** have also shown similar good activity reduction, approximately 65% DNA interaction.

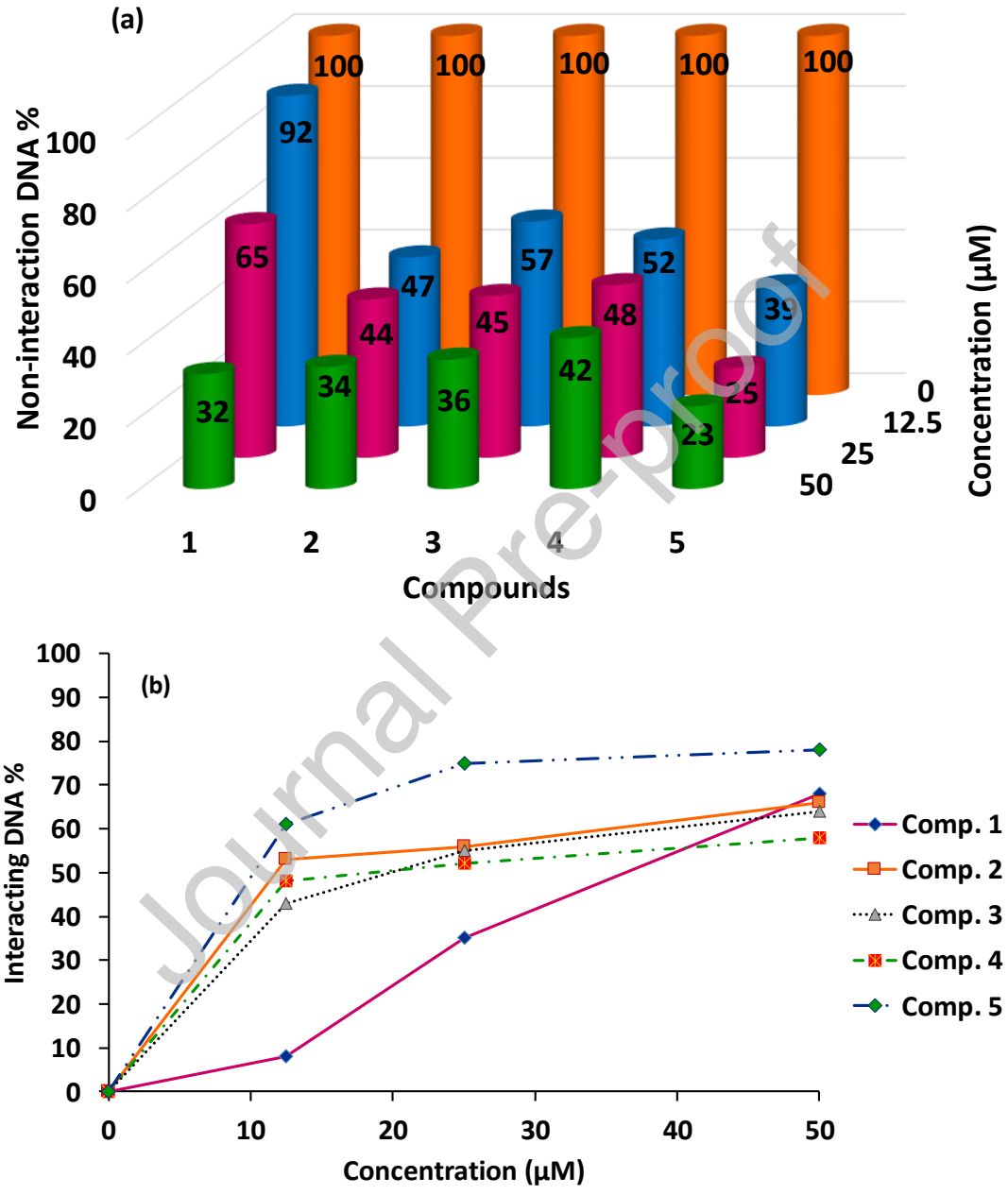

Figure 8. The amperometric responses were shown as percent relative hybridization responses in the figures, indicated by remaining from interaction (**a**) and interacting DNA (**b**). Compounds (0, 12.5, 25 and 50 µM) were incubated with DNA probes prior to the injection on to the biochip.

4. CONCLUSION

In summary, in this study, a series of paraben substituted *s*-triazine compounds were successfully synthesized and DNA interactions of these compounds **1-5** were investigated by an automated biosensor device. The structural properties of all synthesized compounds were examined by MALDI-TOF spectrometer, ^{1}H, ^{13}C NMR spectroscopy. The solid-state structure and geometry of compound **5** was determined using single crystal X-ray structural analysis. In addition, it was confirmed by thermogravimetric analyses (TGA) that all compounds **1-5** showed high thermal stability. Generally, while the parabens interact with DNA at a rate of 35-20%, it was observed that the paraben substituted-s-triazine compounds interact with DNA in approximately 70% at 50 μM concentration. Especially, benzyl-paraben substituted *s*-triazine compound **5**, which the most reactive compound at low concentration, was showed 61% and 75% activity reduction in 12.5 and 25 μM concentrations, respectively. Compound **5** is highly effective in DNA binding activity so, this compound may be a potential candidate as anticancer agents. It is important to quickly determine the effects of drug candidate molecules by pre-screening tests. In this context, data from biosensor analysis studies can help researchers select the most likely drug candidates for further research. In the future application of the study, it is aimed to investigate the anticancer capabilities of the compounds against different cancer cells.

AUTHOR INFORMATION

*Corresponding author: Dr. Elif Şenkuytu

e-mail: elif.senkuytu@atauni.edu.tr , Tel: +90 442 231 4441

SUPPLEMENTARY MATERIAL

Supplementary data were given as Supporting Information. Structure determination has been deposited with the Cambridge Crystallographic Data Centre with references CCDC **1964264**

for compound **5**. These data can be obtained free of charge from The Cambridge Crystallographic Data Centre via www.ccdc.cam.ac.uk/data_request/cif.

Sample CRediT author statement

Elif Şenkuytu: Formal analysis, Writing- Original draft preparation, Supervision.

Derya Davarcı: Investigation and Writing

Zehra Ölçer: Investigation and Writing

Gönül yenilmez Çiftçi: Reviewing and Editing

Declaration of interests

☒ The authors declare that they have no known competing financial interests or personal relationships that could have appeared to influence the work reported in this paper.

ACKNOWLEDGEMENTS

This work was supported by grants from the Gebze Technical University Scientific Research Projects (GTUBAP) (Grant no: BAP 2018-A105-34). We would like to thank BILGEM-TUBITAK for their contribution to the manufacturing of biochip and detection platform.

REFERENCES

[1] Cancer Research WHO, Cancer statistics reports for the WHO. https://www.who.int/news-room/fact-sheets/detail/cancer

[2] The Global Cancer Observatory - All Rights Reserved, (March, 2019). https://gco.iarc.fr/today/data/factsheets/cancers/39-All-cancers-fact-sheet.pdf

[3] F.A. Andersen, Int. J. Toxicol. 27 (2008) 1–82.

[4] M. Fisher, S. MacPherson, J. M. Braun, R. Hauser, M. Walker, M. Feeley, R. Mallick, R. Bérubé, T. E. Arbuckle, Environ. Sci. Technol., 51 (2017) 4009−4017

[5] D. Serbezeanu, I.-D. Carja, A. Nicolescu, M. Aflori, T. Vlad-Bubulac, M. Butnaru, R.-F. Damian, S. Dunca, S. Shova, J. Mol. Struct. 1196 (2019) 637-646.

[6] Y. Nagar, R. S. Thakur, T. Parveen, D. K. Patel, K. R. Ram, A. Satish, Chemosphere 246 (2020) 125730.

[7] M. Shanmugam, K. Narayanan, K. H. Prasad, D. Karthikeyan, L. Chandrasekaran, R. Atchudan, V. Chidambaranathan, New J. Chem., 42 (2018) 1698-1714.

[8] A. El-Faham, M. Farooq, Z. Almarhoon, R. A. Alhameed, M. A.M. Wadaan, B. G. de la Torre, F. Albericio, Bioorg. Chem. 94 (2020) 103397.

[9] D. L. Comins, S. O'Connor, Advances in Heterocyclic Chemistry, New York, 44 (1988).

[10] E. M. Smolin, L. Rapoport, s-Triazine and Derivatives in The Chemistry of Heterocyclic Compounds; New York (1959).

[11] D. Bartholomew, 1,3,5-Triazines. In Comprehensive Heterocyclic Chemistry II, Oxford, 6 (1996) 575.

[12] G. Giacomelli, A. Porcheddu, L. De Luca, Curr. Org. Chem. 8 (2004) 1497–1519.

[13] Y. Xiong, S. Zheng, L. Zhu, H. Guo, F. Yang. J. Mol. Struct. 1164 (2018) 311-316.

[14] L.Stagi, D. Chiriu, M. Scholz, C. M. Carbonaro, R. Corpino, A. Porcheddu, S. Rajamaki, G. Cappellini, R. Cardia, P. C. Ricci, Spectrochim. Acta A Mol. Biomol. Spectrosc. 183 (2017) 348–355.

[15] L. Shao, S. Wang, M. Liu, J. Huang, Y.-N. Liu, Chem. Eng. J., 339 (2018) 509–518.

[16] B. Guo, C. Wu, Q. Su, Z. Liu, X. Li, G. Li, Q. Wu, Mater. Lett. 221 (2018) 236–239.

[17] E. Şenkuytu, E. Tanrıverdi Eçik, B. Çoşut, J. Lumin. 203 (2018) 639–645.

[18] G.S. Ananthnag, J.T. Mague, M.S. Balakrishna, Inorg. Chem. 54 (2015) 10985−10992.

[19] E. Tanrıverdi Eçik, E. Şenkuytu, B. Çoşut, Dyes Pigm. 143 (2017) 455-462.

[20] Y. Xiong, S. Zheng, L. Zhu, H. Guo, F. Yang, J. Mol. Struct. 1164 (2018) 311-316.

[21] Y. Zhang, X. Zeng, L.Mu, Y. Chen, J.-X. Zhang, C. Redshaw, G.Wei, Sens. Actuators B 204 (2014) 24–30.

[22] P. Zassowski, P. Ledwon, A. Kurowska, A.P. Herman, M. Lapkowski, V. Cherpak, Z. Hotra, P. Turyk, K. Ivaniuk, P. Stakhira, G. Sych, D. Volyniuk, J.V. Grazulevicius, Dyes Pigm. 149 (2018) 804–811.

[23] J. Zhou, J.Wang, K. Jin, J. Sun, Q. Fang, Polymer 102 (2016) 301-307.

[24] C.-L. Zhang, Y.-X. Liu, X.-M. Zhang, S. Chen, F. Shen, Y.-H. Xiong, W. Liub, Z.-W. Mao, X.-Y. Le, Mat. Sci. Eng. C 91 (2018) 414–425.

[25] M. Maqbool, A. Manral, E. Jameel, J. Kumar, V. Saini, A. Shandilya, M. Tiwari, N. Hoda, B. Jayaram, Bioorg. Med. Chem. 24 (2016) 2777–2788.

[26] X. Zhou, K. Lin, X. Ma, W.-K. Chui, W. Zhou, Eur. J. Med. Chem. 125 (2017) 1279-1288.

[27] X. Chen, P. Zhan, C. Pannecouque, J. Balzarini, E. D. Clercq, X. Liu, Eur. J. Med. Chem. 51 (2012) 60-66.

[28] D.R. Shah, R.P. Modh, K.H. Chikhalia, Future Med. Chem. 6 (2014) 463-477.

[29] P. Baréa, V. A. Barbosa, D. L. Bidóia, J. C. Paula, T. F. Stefanello, W. F.Costa, C. V. Nakamura, M. H. Sarragiotto, Eur. J. Med. Chem. 150 (2018) 579–590.

[30] S. N. Khattab, H. H. Khalil, A. A. Bekhit, M. M. A. El-Rahman, B. G. Torre, A. El-Faham, F. Albericio, Chem. Med. Chem. 13(7) (2018) 725–735.

[31] A.Shandilya, N. Hoda, S. Khan, E. Jameel, J. Kumar, B. Jayaram, J. Mol. Graph. Model. 71 (2017) 96–10.

[32] A. Sharma, H. Ghabbour, S. T. Khan, B. G. Torre, F. Albericio, A. El-Faham, J. Mol. Struct. 1145 (2017) 244-253.

[33] M. Dinari, F. Gharahi, and P. Asadi, J. Mol. Struct., 1156 (2018) 43–50.

[34] C. Zhou, J. Min, Z. Liu, A. Young, H. Deshazer, T. Gao, Y.-T. Chang, N. R. Kallenbach, Bioorg. Med. Chem. Lett. 18 (2008) 1308–1311.

[35] S. Vembu, S. Pazhamalai, M. Gopalakrishnan, Bioorg. Med. Chem. 23 (2015) 4561–4566.

[36] D. R. Ramadan, A. A. Elbardan, A. A. Bekhit, A. El-Faham, S. N. Khattab, New J. Chem. 42 (2018) 10676–10688.

[37] S. Cascioferro, B. Parrino, V. Span_o, A. Carbone, A. Montalbano, P. Barraja, P. Diana, G. Cirrincione, Eur. J. Med. Chem. 142 (2017) 523-549.

[38] P. Singla, V. Luxami, K. Paul, Eur. J. Med. Chem. 117 (2016) 59-69.

[39] B. Liu, T. Sun, Z. Zhou, L. Du, Med chem 5(3) (2015) 131-148.

[40] S. Cascioferro, B. Parrino, V. Spano, A. Carbone, A. Montalbano, P. Barraja, P. Diana, G. Cirrincione, Eur. J. Med. Chem. 142 (2017) 74-86.

[41] H. Liu, S. Long, K.P. Rakesh, G.-F. Zha, Eur. J. Med. Chem. 185 (2020) 111804.

[42] P. Singla, V. Luxami, K. Paul, Bioorg. Med. Chem. Lett. 26 (2016) 518–523.

[43] A.M. Ismail, S.A. El Sayed, I.S. Butler, S.I. Mostafa, J. Mol. Struct. 1200 (2020) 127088.

[44] J. F. Rusling, E. G. Hvastkovs, J. B. Schenkman, Curr Opin Drug Discov Devel. 10(1) (2007) 67-73.

[45] B. Yang, S. Zhang, X. Fang, J. Kong, Biosens. Bioelectron. 142 (2019) 111544.

[46] F. Kuralay, S. Demirci, M. Kiristi, L. Oksuz, A. U. Oksuz, Colloids and Surfaces B: Biointerfaces 123 (2014) 825–830.

[47] S. Tajik, M.A. Taher, H. Beitollahi, M. Torkzadeh-Mahani, Talanta, 134 (2015) 60-64.

[48] G. Yenilmez Çiftci, E. Şenkuytu, S.E. Incir, F. Yuksel, Z. Olcer, T.Yildirim, A. Kilic, Y. Uludag, Biosens. Bioelectron. 80 (2016) 331-338.

[49] A. Rescifina, U. Chiacchio, A. Corsaro, A. Piperno, R. Romeo, Eur. J. Med. Chem. 46 (2011) 129-136.

[50] Bruker (2007) APEX2, Bruker AXS Inc., Madison, Wisconsin, USA.

[51] Bruker (2007) SAINT, Bruker AXS Inc., Madison, Wisconsin, USA.

[52] Bruker (2001) SADABS, Bruker AXS Inc., Madison, Wisconsin, USA.

[53] G. M. Sheldrick, Acta Cryst., A71 (2015) 3-8

[54] G. M. Sheldrick, Acta Cryst., C71, (2015) 3-8.

[55] O.V. Dolomanov, L.J. Bourhis, R.J. Gildea, J.A.K. Howard, H. Puschmann, J. Appl. Cryst., 42 (2009) 339-341

[56] A. L. Spek, Acta Cryst. D65 (2009) 148-155.

[57] C. F. Macrae, P. R. Edgington, P. McCabe, E. Pidcock, G. P. Shields, R. Taylor, M. Towler, J. van de Streek, J. Appl. Cryst., 39 (2006) 453-457.

[58] CODEN: JKXXAF JP 62178576 A 19870805; Application: JP 86-20610 19860131. Priority: CAN 108:37873 AN 37873, 1988.

[59] E. Şenkuytu, T. Yıldırım, Z. Ölçer, Y. Uludağ, G. Yenilmez Çiftçi, Inorg. Chim. Acta 477 (2018) 219–226.

[60] D. Serbezeanu, I.-D. Carja, A. Nicolescu, M. Af. T. Vlad-Bubulac, M. Butnaru, R.-F. Damian, S. Dunca, S. Shova, J. Mol. Struct. 1196 (2019) 637-646.

[61] D. Dubey, D. Chopra, J. Singh, A. K. Srivastav, S. Kumari, A. Verma, R.S. Ray, Food Chem. Toxicol. 108 (2017) 171-185.

[62] J. Roszak, A. Smok-Pieniążek, K. Domeradzka-Gajda, J. Grobelny, E. Tomaszewska, K. Ranoszek-Soliwoda, G. Celichowski, M. Stępnik, Toxicol. and App. Pharm. 337 (2017) 12–21.

[63] V. R. Thalladi, S. Brasselet, H-C. Weiss, D. Bla1ser, A. K. Katz, H. L. Carrell, R. Boese, J. Zyss, A. Nangia, and G. R. Desiraju, J. Am. Chem. Soc. 120 (1998) 2563-2577.

[64] A. Barakat, F.F. El-Senduny, Z. Almarhoon, H. H. Al-Rasheed, F. A. Badria, A. M. Al-Majid, H. A. Ghabbour, and A. El-Faham, J. Chem. (2019) 9403908.

[65] A. C. Larson, D. T. Cromer, J. Chem. Phys. 60 (1974)185-192.

[66] B. Ju1rgens, E. Irran, J. Schneider, and W. Schnick, Inorg. Chem. 39 (2000) 665-670.

[67] D. Cremer and J. A. Pople, J. Am. Chem. Soc. 1975, 97, 1354–1358.

[68] A. L. Spek, Acta Cryst. D65 (2009) 148-155

[69] A. L. Spek. Acta Cryst., C71, (2015) 9-18.

[70] G. Yenilmez Çiftçi, E. Şenkuytu, S.E. İncir, E.T. Eçik, Y. Zorlu, Z. Olcer, Y. Uludag, Microchim Acta 184 (2017) 2307-2315.

[71] E. Palecek, M. Fojta, M. Tomschik, J. Wang, Biosens. Bioelectron. 13 (1998) 621–628.

[72] E. Şenkuytu, P. Kızılkaya, Z. Ölçer, U.Pala, D. Davarcı, Y. Zorlu, H. Erdoğan, G. Yenilmez Çiftci, Inorg. Chem. 59 (2020) 2288−2298.